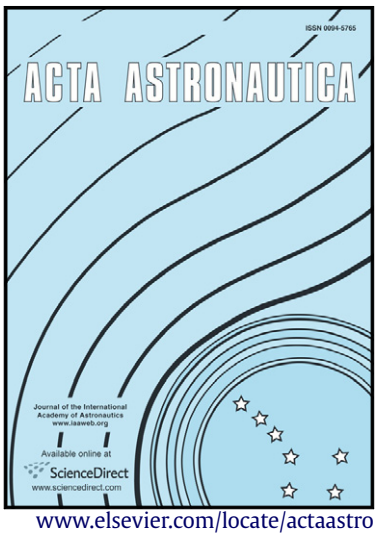

www.elsevier.com/locate/actaastro

Chaos and its avoidance in spinup dynamics of an axial dual-spin spacecraft

Anton V. Doroshin

PII: S0094-5765(13)00346-9
DOI: http://dx.doi.org/10.1016/j.actaastro.2013.09.003
Reference: AA4855

To appear in: *Acta Astronautica*

Received date: 14 April 2013
Revised date: 6 September 2013
Accepted date: 11 September 2013

Cite this article as: Anton V. Doroshin, Chaos and its avoidance in spinup dynamics of an axial dual-spin spacecraft, *Acta Astronautica,* http://dx.doi.org/10.1016/j.actaastro.2013.09.003

CHAOS AND ITS AVOIDANCE IN SPINUP DYNAMICS OF AN AXIAL DUAL-SPIN SPACECRAFT

Anton V. Doroshin

Space Engineering Department (Division of Flight Dynamics and Control Systems),
Samara State Aerospace University (National Research University),
SSAU, 34, Moskovskoe Shosse str., Samara, 443086, Russia

E-mail: doran@inbox.ru

Abstract. Attitude dynamics of a dual-spin spacecraft (DSSC) and a torque-free angular motion of a coaxial bodies system are considered. Some regimes of the heteroclinic chaos are described. The local chaotization of the DSSC is investigated at the presence of polyharmonic perturbations and small nutation restoring/overturning torques on the base of the Melnikov method and Poincaré Maps. Reasons of the chaotic regimes initiation at the spinup maneuver realization are studied. An approach for the local heteroclinic chaos escape/avoidance at the modification of the classical spinup maneuver is suggested.

Keywords: Dual-spin Spacecraft, Dual-spin satellite, Gyrostat, Homoclinic Chaos, Polyharmonic Perturbations, Nutation Restoring/Overturning Torques, Melnikov Function, Poincaré Map.

INTRODUCTION

The study of the angular motion of coaxial rigid bodies systems and dual-spin spacecraft (DSSC) attitude dynamics is one of the main problems of rigid body systems mechanics [1-41].

Tasks of the analysis/synthesis of the coaxial bodies' motion have important applications in the spaceflight dynamics and corresponding space missions which include orbital path sections with the attitude stabilization of the DSSC [8-16]. The DSSC consists of two coaxial bodies, rotating about a common axis (freely or at the presence of the internal engine torques).

The dual-spin construction-scheme is quite useful in the practice during the history of the space flights realization; and it is possible to present some examples of the DSSC, which was used in real space-programs (most of them are communications dual-spin satellites and observing geostationary satellites).

This is the long-continued and well successful project "Intelsat" (the Intelsat II series of satellites first launched in 1966) including the 8th generation of geostationary communications satellites and the Intelsat VI (1991) designed and built by Hughes Aircraft Company. Also one of the famous Hughes' DSSC is the experimental tactical communications dual-spin satellite TACSAT-I which was launched into synchronous orbit in 1969. The "Meteosat"- project by European Space Research Organization (initiated with the Meteosat-1 in 1977 and operated until 2007 with the Meteosat-7) also used the dual-spin configuration spacecraft. The spin-stabilized spacecraft with mechanically despun antennas was applied in the framework of GEOTAIL (the collaborative mission of Japan JAXA/ISAS and NASA, within the program "International Solar-Terrestrial Physics") launched in 1992; the GEOTAIL spacecraft and its payload continue to operate in 2013. Analogously the construction scheme with the despun antenna was selected for Chinese communications satellites DFH-2 (STW-3, 1988; STW-4, 1988; STW-55, 1990). The well-known Galileo mission's spacecraft (the fifth spacecraft to visit Jupiter, launched on October 19, 1989) was designed by the dual-spin scheme. Of course, we should indicate one of the world's most-purchased commercial communications satellite models such as Hughes / Boeing HS-376 / BSS-376 (for example, the "Satellite Business Systems" with projects SBS-1, 2, 3, 4, 5, 6 / HGS-5, etc.): they have spun sections containing propulsion systems, solar drums, and despun sections containing the satellite's communications payloads and antennas. Also very popular and versatile dual-spin models are the Hughes' HS-381 (the Leasat project), HS-389 (the Intelsat project), HS-393 (the JCSat project).

The DSSC usually is used for the attitude stabilization by the partial twist method: only one of the DSSC's coaxial bodies (the «rotor»-body) has rotation at the «quiescence» of the second

body (the «platform»-body) – it allows to place into the «platform»-body some exploratory equipment and to perform of space-mission tests without rotational disturbances. Moreover, one of the widespread types of the DSSC is the axial DSSC, where the axisymmetric rotor is aligned with the principal axis of the platform-body.

The investigation of the motion chaotic regimes is also the significant part of the research into DSSC attitude dynamics. Here we can indicate many works, e.g. [18-27]. Analysis of the angular motion of the coaxial bodies with the variable structure was carried out in [19, 36-38]. In [18] the motion chaotization of a rigid body with a rotor attachment was studied based on the Melnikov method's modification using the classical heteroclinic solutions for the single rigid body torque-free angular motion. In [12-16] DSSC tilting motion's evolutions at the rotor's spinup maneuver realization was in details investigated with the help of direct integration of dynamical equations.

As it is described in the previous works, e.g. [15], the DSSC are usually placed into the orbit with zero relative rotor angular velocity, and then a spinup engine provides an internal torque from the «platform»-body to the «rotor»-body along the common rotation axis of the DSSC's coaxial bodies. The effect of the axial torque is to spin up the rotor and despin the platform, thereby transferring all or most of the angular momentum to the rotor. Usually the spinup torque is constant; also this torque is switched off right after the angular momentum transferring. However, for maintaining of the constancies of the rotor's relative angular velocity the DSSC's control system can form the corresponding stabilizing internal torque. This scheme of the angular momentum translation (from the platform-body to the rotor-body) is called as the classical spinup maneuver.

During this maneuver the DSSC's longitudinal axis can be captured in the tilting precessional motion with the complex time-dependence of the nutation angle – it corresponds to the space mission disruption. Here we also note that at this spinup maneuver the «platform»-body move from quite high-velocity rotations to slow oscillations. By this reason the DSSC's dynamical system passes through the separatrix-trajectory in the corresponding phase-space [12-16].

In an extension of the indicated works [9-38] in this research on the base of the Melnikov method we consider the complex tilting precessional motion's initiation as the realization of the chaotic regimes close to the heteroclinic separatrix-trajectory at the presence of small internal perturbations in the rotor's spinup-engine. Also the new scheme of the spinup maneuver realization is suggested – this scheme can immediately translates the gyroscopic stabilizing angular momentum to the rotor-body without chaotic regimes arising.

At the end of the introduction-section we can shortly indicate some important facts about the DSSC and its possible chaotic behavior. So, the dual-spin satellites usually are used in communication systems. The average lifetime (the design service life) of the DSSC is 10 years, but some practical cases are known which exceeded the contractual lifetime by more than 20 years. The dual-spin satellites, as well as other types of satellites, are affected by many external and internal influences, so the various failures are possible. The appropriate analysis of the failures rate/source was made by different organizations and authors, e.g. [42-44]. The failures/anomalies have been reclassified [43] into six categories: (1) Mission Failure, (2) Random Part Failure, (3) Degraded Performance, (4) Phantom Commands, (5) Spurious Signals, and (6) Command Errors. In the framework of the stated problem of the chaotic DSSC modes investigation the most interesting anomalies are connected with phantom commands and spurious signals. It is quite possible that some of the listed implementations of "the phantom commands" (uncommanded reconfigurations of the vehicles) [43] can be considered as the realizations of the unidentified chaotic regimes in the dual-spin satellites' dynamics. These are "loss of earth lock and spin-up" (DSCS-2), "despun platform spun up" (INTELSAT-3), "loss of despin control caused despin platform to drive off the earth" (INTELSAT-4), "despin electronics control switched automatically" (TAC COMSAT), also anomalies into the attitude control electronics [44] in cases of such DSSC as the AUSSAT-A3 and the SBS-1. All of the indicated and similar accidents constitute the problem of the chaotic DSSC motion which is partially considered in this article.

1. The DSSC angular motion equations

Let's consider the torques-free angular motion of the axial DSSC (the body #1 is the rotor; the body #2 is the platform). The platform-body has the general inertia tensor and the rotor-body is dynamically symmetrical. The DSSC motion is considered in the inertial coordinate system *OXYZ* (fig.1). We can describe corresponding attitude dynamics in terms of the Euler angles [1, 2] and/or on the base of well-known Andoyer-Deprit (also called as Serret-Andoyer) variables [3-5]. We assume the following inertia moments ratio $A_2 > B_2 > C_2 > A_1 > C_1$.

The system's motion equation can be written in the form [26]:

$$\begin{aligned} &A\dot{p} + (C_2 - B)qr + q\Delta = 0; \quad B\dot{q} + (A - C_2)pr - p\Delta = 0; \\ &C_2\dot{r} + \dot{\Delta} + (B - A)pq = 0; \quad \dot{\Delta} = M_\Delta, \end{aligned} \tag{1.1}$$

where $[p, q, r]^T$ – are components of the absolute angular velocity of the main body (the platform-body) in the connected frame $Ox_2y_2z_2$, σ – the relative angular velocity of the rotor-body; $\Delta = C_1(r + \sigma)$; $A = A_1 + A_2$, $B = A_1 + B_2$; $diag[A_1, A_1, C_1]$, $diag[A_2, B_2, C_2]$ – are the inertia tensors of the coaxial bodies (## *i*=1, 2) in the corresponding connected frames $Ox_iy_iz_i$, M_Δ – the internal torque of the rotor-engine.

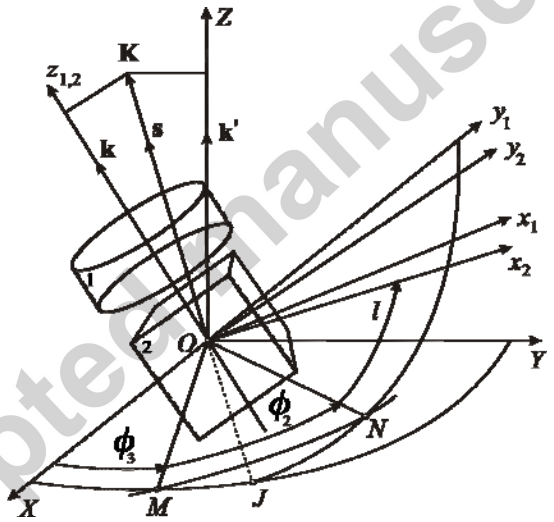

Fig.1 *The coaxial bodies (the axial DSSC)*

The Andoyer-Deprit variables [3, 4] are defined as follows (fig.1):

$$L = \frac{\partial T}{\partial \dot{l}} = \mathbf{K}\cdot\mathbf{k}; \; I_2 = \frac{\partial T}{\partial \dot{\varphi}_2} = \mathbf{K}\cdot\mathbf{s} = |\mathbf{K}| = K; \; I_3 = \frac{\partial T}{\partial \dot{\varphi}_3} = \mathbf{K}\cdot\mathbf{k}'; \quad L \le I_2$$

$$K_{x_2} = Ap = \sqrt{I_2^2 - L^2}\sin l; \; K_{y_2} = Bq = \sqrt{I_2^2 - L^2}\cos l; \; K_{z_2} = C_2 r + \Delta = L, \tag{1.2}$$

where $\mathbf{K}$ is the vector of the DSSC angular momentum. In the Andoyer-Deprit variables we have the well-known Hamiltonian form:

$$H = H_0 + \varepsilon H_1; \quad H_0 = T = \frac{I_2^2 - L^2}{2}\left[\frac{\sin^2 l}{A_1 + A_2} + \frac{\cos^2 l}{A_1 + B_2}\right] + \frac{1}{2}\left[\frac{\Delta^2}{C_1} + \frac{(L - \Delta)^2}{C_2}\right], \tag{1.3}$$

where *T* is the system kinetic energy, H_1 – the perturbed part of the Hamiltonian and ε – the small parameter corresponding to perturbations.

The coordinates φ_2, φ_3 miss in the Hamiltonian (1.3), then the corresponding conjugate momentums are constant, and the dynamical system reduced to the one-degree-of-freedom subsystem $\{l, L\}$ [26, 27, 32, 33]:

$$\dot{L} = f_L(l,L) + \varepsilon g_L(t); \qquad \dot{l} = f_l(l,L) + \varepsilon g_l(t)$$

$$f_L(l,L) = -\frac{\partial H_0}{\partial l} = \alpha\left(I_2^2 - L^2\right)\sin l\cos l$$

$$f_l(l,L) = \frac{\partial H_0}{\partial L} = L\left[\frac{1}{C_2} - \frac{\sin^2 l}{(A_1+A_2)} - \frac{\cos^2 l}{(A_1+B_2)}\right] - \frac{\Delta}{C_2} \tag{1.4}$$

$$g_L = -\frac{\partial H_1}{\partial l}; \quad g_l = \frac{\partial H_1}{\partial L}$$

where g_l, g_L – are the perturbations, and $\alpha = (A_1+B_2)^{-1} - (A_1+A_2)^{-1}$.

2. Perturbations of the DSSC attitude motion

Let's consider the DSSC motion at the initiation of the small polyharmonic perturbation between the coaxial bodies after the spinup maneuver's implementation $(\Delta = \bar{\Delta} = \text{const})$

$$\dot{\Delta} = M_\Delta = \varepsilon\sum_{n=0}^{N}\left[a_n \sin nt + b_n \cos nt\right] \tag{2.1}$$

With the help of the polyharmonic form (2.1) we can simulate arbitrary decomposable in finite Fourier series (with N expansion terms) internal torques corresponding to the complex impulse signals in the DSSC control system, including spurious currents at the presence of latency in the rotor angular velocity sensors.

After the eq. (2.1) integration we obtain the polyharmonic solution form:

$$\Delta = \bar{\Delta} + \varepsilon\sum_{n=0}^{N}\left[\bar{a}_n \sin nt + \bar{b}_n \cos nt\right] \tag{2.2}$$

The substitution of (2.2) into eq. (1.4) gives us the perturbed dynamical system:

$$\dot{L} = f_L(l,L) + \varepsilon g_L(t); \quad \dot{l} = f_l(l,L) + \varepsilon g_l(t);$$

$$f_L(l,L) = \alpha\left(I_2^2 - L^2\right)\sin l\cos l; \quad f_l(l,L) = L\left[\frac{1}{C_2} - \frac{\sin^2 l}{(A_1+A_2)} - \frac{\cos^2 l}{(A_1+B_2)}\right] - \frac{\bar{\Delta}}{C_2}; \tag{2.3}$$

$$g_L(t) = 0; \quad g_l(t) = -\eta\sum_{n=0}^{N}\left[\bar{a}_n \sin nt + \bar{b}_n \cos nt\right]; \quad \eta = \frac{1}{C_2}$$

Also the perturbation form (2.3) is actual at the presence of the small potential (*P*) corresponding to small external "nutation" restoring/overturning torques with the polyharmonic amplitude $\zeta(t)$:

$$\zeta(t) = \varepsilon\sum_{n=0}^{N}\left[\bar{a}_n \sin nt + \bar{b}_n \cos nt\right];$$

$$P = \zeta(t)\cos\theta = \varepsilon\sum_{n=0}^{N}\left[\bar{a}_n \sin nt + \bar{b}_n \cos nt\right]\cos\theta;$$

$$H_1 = \cos\theta\sum_{n=0}^{N}\left[\bar{a}_n \sin nt + \bar{b}_n \cos nt\right];$$

$$g_L(t) = 0; \quad g_l(t) = -\frac{\partial H_1}{\partial L}$$

Here we note that the nutation angle θ (the angle between longitudinal DSSC's axis and the selected direction in the inertial space) can be counted out from the system angular moments' direction (fig.1) [26, 34], and then we will have the following expressions

$$\cos\theta = \frac{L}{I_2}; \quad g_L(t) = 0; \quad g_l(t) = -\tilde{\eta}\sum_{n=0}^{N}\left[\bar{a}_n \sin nt + \bar{b}_n \cos nt\right]; \quad \tilde{\eta} = \frac{1}{I_2}$$

3. The Melnikov function evaluation

As it was indicated in the introduction section, the spinup maneuver includes the passing through the separatrix-trajectory in the system's phase space. During this process the DSSC's longitudinal axis can be captured in tilting precessional regimes with complex time-dependences of the nutation angle. This effect can be explained on the base of the local chaotization of the DSSC motion close to the separatrix-trajectory.

First of all, we present examples of the unperturbed phase portrait (fig.2-a) and the phase portrait (fig.2-b) of the system at the perturbations (2.3) in the Andoyer-Deprit phase space corresponding to the Poincaré section.

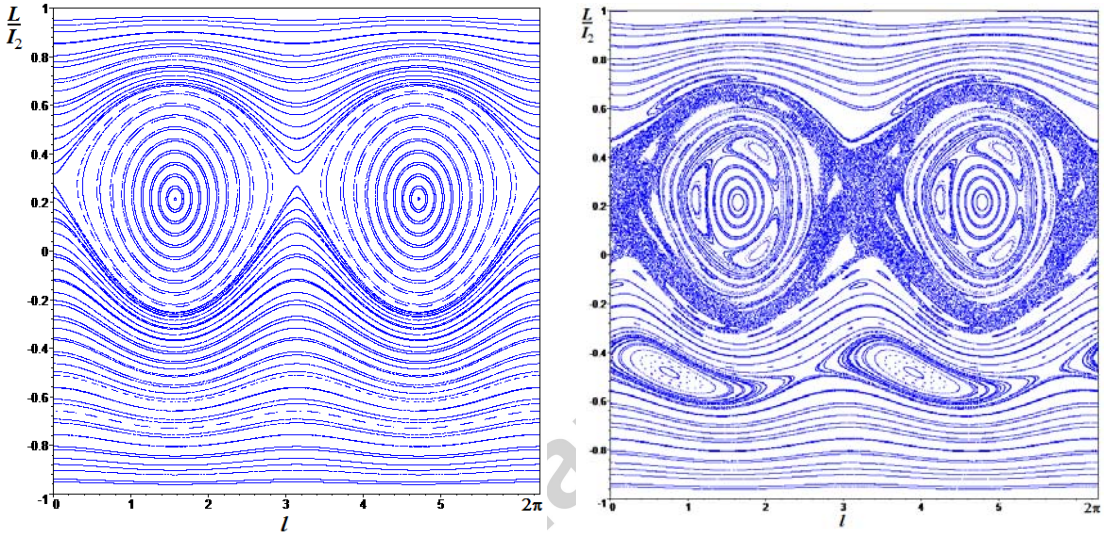

(a) (b)

Fig.2 *The Poincaré section:* $A_2 = 15,\ B_2 = 8,\ C_2 = 6,\ A_1 = 5,\ C_1 = 4;\quad I_2 = 20;\quad \bar{\Delta} = 3:$
a). $\varepsilon = 0;$ b). $\varepsilon = 0.3;\ \eta = 1/6;\ \bar{a}_3 = 1$

The presented (fig.2) examples of the Poincaré sections were plotted in the case of the single-harmonic perturbation $\left(\bar{a}_j = \bar{b}_j = 0\ \ \forall j \neq 3\right)$ on the base of the following "oscillations-phase-repetition" section-condition: $\left(3t \bmod 2\pi\right) = 0$. As can we see, at the presence of the perturbation the "chaotic layer" formed in the region close to the heteroclinic separatrix-trajectory. This chaotic layer is generated as the result of multiple intersections of the stable and unstable split manifolds of the heteroclinic separatrix-trajectory. Inside the chaotic layer phase trajectories can performed complex "chaotic" evolutions including complicated alternations of rotating and oscillating regimes with variable characteristics – it is the main reason of the DSSC capture in the complex tilting motion.

To analyze the indicated possibility of the local motion chaotization we can use the well-known Melnikov method [17]. For using of this method it is needed to obtain corresponding exact explicit heteroclinic dependences. In this research we will use the heteroclinic solutions obtained in the work [26]:

$$\bar{p}(t)=\pm\sqrt{\frac{C_2(B-C_2)}{A(A-B)}}y(t);\quad \bar{q}(t)=\pm\sqrt{s^2-k^2\left(y(t)+\Delta\beta\right)^2};\quad \bar{r}(t)=y(t)+\frac{\bar{\Delta}}{B-C_2};$$

$$y(t)=\frac{4a_0E\left(y_0^{\pm}\right)\exp\left(\mp\dfrac{M\sqrt{a_0}}{k^2}t\right)}{\left[E\left(y_0^{\pm}\right)\exp\left(\mp\dfrac{Mt\sqrt{a_0}}{k^2}\right)-a_1\right]^2-4a_2a_0}, \tag{3.1}$$

where

$T=kinetic\,energy\,level;\quad \bar{\Delta}=\text{const}>0;\ a_2=-k^2;\ a_1=-2\Delta\beta k^2;\ a_0=s^2-k^2\Delta^2\beta^2;$

$$y_0^{\pm}=\pm\frac{s}{k}-\Delta\beta;\quad \beta=(B-C_2)^{-1}-(A-C_2)^{-1};\ E(z)=\frac{2a_0+a_1z+2\sqrt{a_0}\sqrt{a_2z^2+a_1z+a_0}}{z};$$

$$s^2=\frac{H}{B(A-B)};\quad k^2=\frac{C_2(A-C_2)}{B(A-B)};\quad H=2T\left(A-\tilde{D}\right)+\Delta^2b;\quad \tilde{D}=\frac{\Delta^2a}{2T}+B;$$

$$M=\frac{(A-C_2)}{B}\sqrt{\frac{C_2(B-C_2)}{A(A-B)}};\quad a=\frac{C_1C_2+(B-C_2)(C_1-B)}{(B-C_2)C_1};\ b=\frac{C_2C_1+(A-C_2)(C_1-A)}{(A-C_2)C_1}.$$

The Melnikov function in the considered case (for the system (2.3)) has the form:

$$M(t_0)=\varepsilon\int_{-\infty}^{+\infty}f_L\left(\bar{p}(t),\bar{q}(t),\bar{r}(t)\right)g_l(t+t_0)\,dt \tag{3.2}$$

where taking into account expressions (1.4) and with the help of (1.2) we can rewrite the function f_L

$$f_L\left(\bar{p}(t),\bar{q}(t),\bar{r}(t)\right)=f_L\left(\bar{l},\bar{L}\right)=\alpha\left(I_2^2-L^2\right)\sin l\cos l=\alpha A\bar{p}(t)B\bar{q}(t)$$

Then the Melnikov function is evaluated as follows:

$$M(t_0)=\varepsilon\alpha\eta\int_{-\infty}^{+\infty}A\bar{p}(t)B\bar{q}(t)\sum_{n=0}^{N}\left[\bar{a}_n\sin n(t+t_0)+\bar{b}_n\cos n(t+t_0)\right]dt=$$

$$=\varepsilon\alpha\eta\sum_{n=0}^{N}\left[J_s^{(n)}\left\{\bar{a}_n\cos nt_0-\bar{b}_n\sin nt_0\right\}+J_c^{(n)}\left\{\bar{a}_n\sin nt_0+\bar{b}_n\cos nt_0\right\}\right],$$

where

$$J_s^{(n)}=\int_{-\infty}^{+\infty}\bar{g}(t)\sin(nt)\,dt;\ J_c^{(n)}=\int_{-\infty}^{+\infty}\bar{g}(t)\cos(nt)\,dt; \tag{3.3}$$

$$\bar{g}(t)=AB\bar{p}(t)\bar{q}(t)=\pm AB\sqrt{\frac{C_2(B-C_2)}{A(A-B)}}\sqrt{s^2-k^2\left(y(t)+\Delta\beta\right)^2}\,y(t)$$

It is easy to show that the function $\bar{g}(t)$ is an odd-function exponentially damped to the zero-value at $t\to\pm\infty$. So, by this reason we have convergent improper integrals (3.3) with the following corresponding constant values:

$$J_c^{(n)}=0;\quad J_s^{(n)}=\text{const}_n \tag{3.4}$$

Having in the mind constants (3.4) we obtain the polyharmonic form of the Melnikov function:

$$M(t_0)=\varepsilon\alpha\eta\sum_{n=0}^{N}J_s^{(n)}\left\{\bar{a}_n\cos nt_0-\bar{b}_n\sin nt_0\right\} \tag{3.5}$$

The polyharmonic form (3.5) allows us to conclude that the Melnikov function almost always has the infinity quantity of the simple zero-roots (with the exception of some separate cases of the parameters $\left\{\bar{a}_n,\bar{b}_n,J_s^{(n)}\right\}_{n=1..N}$ combinations). It proves the fact of multiple intersections of the stable and unstable split manifolds of the heteroclinic separatrix-trajectory and, therefore, the

fact of the local heteroclinic chaos initiation.

Thus, as showed with the help of the Melnikov function, practically in all cases of perturbations the DSSC dynamics is liable to the local heteroclinic chaotization, which is the main reason of the tilting motion with the corresponding disruption of the space mission.

4. Additional aspects of the realization of the spinup maneuver

To understanding of the DSSC chaotization's features we need to consider some details of the spinup maneuver's realization [12-16].

First of all, the aim of the maneuver is the creation of the DSSC gyroscopic momentum for the attitude stabilization with the help of the rotation of only the rotor-body ("the partial twist" [12-16, 35-38]). The stabilized direction of the DSSC (its longitudinal axis) in ideal conditions coincides with the direction of the angular momentum's vector of the system. In real conditions, certainly, some small misalignments of the angular momentum direction and the DSSC's longitudinal axis take place (the angular momentum vector is the main direction in the space) – this difference corresponds to the nutation angle: $\theta = \angle(\mathbf{k},\mathbf{s})$ (fig.1). So, the DSSC's partial-twist-stabilization provides its attitude orientation with the small defined nutation angle $(\bar{\theta})$. Also we have to indicate, that in this case the following correspondences between classical Euler's angles and Andoyers'–Deprit's variables take place [34]:

$$\cos\theta = L/I_2;\ \ l = \varphi \tag{4.1}$$

where φ is the platform-body's intrinsic rotation angle.

In the second place, during this maneuver the angular momentum is transporting from the platform-body to the rotor-body, and by this reason the absolute longitudinal angular momentum of the platform-body is reducing to the zero-value $(C_2 r_0 \to 0)$, and at the end of the maneuver the rotor-body receives all the system initial absolute longitudinal angular momentum $(C_1 r_0 \to L_0)$.

Let's consider the spinup maneuver's realization as the series of small separated steps with the graceful increment of the Δ-value, which occurs under the action of the internal torque of the rotor-spinup-engine. In this aspect of the maneuver consideration we take the series of the systems' independent phase portraits (the frames set), corresponding to the series of Δ-values. We can show some important frames of the phase portraits[1] variation (fig.3). Here we note that the defined stabilizing value of the nutation angle (and the corresponding particular solution) is depicted as the red curve (fig.3).

As can we see, during the Δ-value increasing the separatrix-region (the saddle points and corresponding heteroclinic separatrices) is gradually moving up at the phase plane (fig.3: frames a-e). Herewith, the separatrix saddle points coincides with the stabilizing-nutation-angle particular solution (frame d), and, at the continued increasing of the Δ-value the separatrix-region breaks through (bottom-to-up) the stabilizing particular solution (frame e). Following further, the separatrix-region rises up, and the saddle-points coincide with the upper level of the phase space (frame f) – this corresponds to the «critical» Δ*-value [26, 27]. After this the rising up of the separatrix-region is continued (frame g) with the overcritical Δ-values, and, finally, the separatrix-region fully vanishes (frame h) at the secondary critical Δ**-value. Here we note that the following magnitudes correspond to the critical values:

$$\begin{gathered}\Delta^* = K(B-C_2)/B = K\beta; \qquad \Delta^{**} = K(A-C_2)/A = K\alpha \\ \alpha = 1-\frac{C_2}{A};\quad \beta = 1-\frac{C_2}{B};\quad 0<\beta<\alpha<1;\quad 0<\Delta^*<\Delta^{**}<K=I_2\end{gathered} \tag{4.2}$$

[1] At this and other following figures we have for the phase portraits the dimensionless system axes: the abscissa corresponds to the angle l [rad], and the ordinate corresponds to the dimensionless L/I_2-ratio (whereas (4.1) this coordinate plane $\{l, L/I_2\}$ is conformed to $\{\varphi, \cos\theta\}$; the phase structure corresponds to the nutation-angle changing). So, we will not write notations of coordinate systems' axes at the phase-portrait-figures.

We can conclude that the separatrix-region inevitably intersects the particular solution of the stabilizing-nutation-angle [16]; this intersection occurs between frames c-e (fig.3). By this reason we have the inevitable passage of the stabilizing-nutation-angle solution through the local heteroclinic chaotic area (fig.3, frames a'-g'). This fact confirms the guaranteed capture of the DSSC into the local chaotic regime (in [16] is indicated that there are probability phenomena of various outcomes of the DSSC evolution at the separatrix crossing). It is worth to note that in the case of small perturbations this chaotic regime can be expressed in a very weak form, which hides its fundamental presence in the DSSC dynamics, especially in the practical implementation of well-proven space missions (with minimal errors and perturbations). So, the chaotization aspects in the DSSC's perturbed dynamics always take place, and it can always become the main reason for the DSSC's attitude disorientation and, moreover, for the disruption of the space mission.

Separately we need to describe the phase portraits connected with the frames h and h' (fig.3). As it was indicated, the heteroclinic separatrix-region fully vanishes at the values $\Delta \geq \Delta^{**}$ – this circumstance eliminates all reasons for the local heteroclinic chaos generation (though some complication of the phase portrait's (fig.3-h') structure occurs). This case is most favorable for the DSSC attitude stabilization, but it can be implemented only at the end of the classical spinup maneuver's realization. It is also necessary to note, that the smaller the internal torque of the rotor's spinup, the more gradual is the transition to the finite case (h/h'), and the more stable is the chaotic regime. If the spinup maneuver were discrete and could instantly translate the whole longitudinal angular momentum of the platform-body to the rotor-body (the instantaneous transition to the case h/h'), then the reasons for the local heteroclinic chaos would be fully eliminated.

For the numerical examples (fig.3) of the system (2.3) behavior we used the following parameters (Δ-frame-values are presented in the table):

$A_2 = 15,\ B_2 = 8,\ C_2 = 6,\ A_1 = 5,\ C_1 = 4$ [kg·m^2]; $I_2 = 20$ [kg·m^2/s];

$\eta = 1/6\ \left[\left(\text{kg}\cdot\text{m}^2\right)^{-1}\right];\ \bar{a}_1 = 1;\ \bar{a}_{2..N} = \bar{b}_{0..N} = 0\ \left[\text{kg}\cdot\text{m}^2/\text{s}\right];\ \cos\bar{\theta} = 0.8.$

The small parameter: the left column corresponds to $\varepsilon = 0$; the right column - $\varepsilon = 0.3$.

The Poincaré sections' condition: $(t \bmod 2\pi) = 0$.

Table

Frame	a, a'	b, b'	c, c'	d, d'	e, e'	f, f'	g, g'	h, h'
Δ, kg·m^2/s	0	5	8	8.62	9	Δ^*=10.77	13	Δ^{**}=14

Also it is worth to underscore some differences in the chaos regimes, which arise during the spinup maneuver. The indicated differences are presented at the fig.4.

First of all, at the relatively "small" Δ-values $\left(0 < \Delta < \Delta^*\right)$ we see (fig.4-a) the broad chaotic layer spreading on the wide zone of the nutation oscillations ($\cos\theta$ is changing inside the interval, which includes both negative and near-unit values, therefore the nutation-angle can oscillate with big amplitudes from near-zero magnitudes up to the values above π/2). In this case the longitudinal DSSC-axis performs chaotic tumbling-evolutions. We can define this chaotic regime as the "oscillating chaos".

The second type of the chaos regimes (fig.4-b) corresponds to the overcritical Δ-values $\left(\Delta^* \leq \Delta < \Delta^{**}\right)$, when the motion occurs in the "upper" zone of the phase space $\left(0 < \cos\theta \leq 1\right)$. In this case the rotation of the DSSC longitudinal axis about angular momentum's direction preferably takes place, when the chaotic regime resembles the gyroscope regular precession (certainly with the chaotic amplitude). We can define this chaotic regime as the "rotating chaos". This case is less dangerous for the DSSC's attitude stabilization than the oscillating chaos.

The third case of the chaos regimes is possible. This is the heteroclinic chaos close to the secondary heteroclinic structures arising in addition to the main separatrix-region at the presence

of perturbations (fig.4-c). These secondary heteroclinic bundles usually are quite narrow (along the ordinate-direction) and have properties similar to the rotational chaos. The figure (fig.4-c) demonstrates the narrow secondary chaotic bundle at the value Δ^{**}, when the main separatrix-region is already vanished. This type of the chaotic regime we can define as the "secondary chaos".

Also as can we see (fig.4-d), the absence of any chaotic regimes is possible at large Δ-values comparable with the value of the system angular momentum ($\Delta \sim 0.9 \cdot I_2$). It is quite clear, because in this case the greater part of the system's angular momentum is transferred to the dynamically-symmetrical rotor-body and the platform-body with the three-axial inertia tensor is almost motionless in the inertial space, and therefore the DSSC dynamics is determined by the simple dynamics of the dynamically-symmetrical rotor. This case of the motion is most preferred to the DSSC's attitude stabilization. The implementation of the "chaos-free" phase portrait (fig.4-d) is possible if the initial DSSC's attitude orientation is quite precise and the nutation-angle's initial value is quite small – then after the spinup maneuver the longitudinal angular momentum will be fully transferred to the rotor-body with the appropriate large value of the angular momentum Δ (in the considered at the fig.4-d example the nutation-angle corresponds to the condition: $\cos\theta = \Delta / I_2 = 0.9$).

In an addition to the Poincaré-maps (fig.3,4) we present illustrations of the chaotic motion with the help of the time-history of the angular velocity's components (fig.5-a), the perturbed polhode (in the *p*-*q*-*r*-space of the angular moment's ellipsoid) and the corresponding Poincaré-map (fig.5-b), the time-history of the nutation angle (fig.5-c), the time-history of the intrinsic rotation angle (fig.5-d), the six Poincaré-maps-images of the unperturbed heteroclinic separatrix in the forward-time-direction $t \to +\infty$ (fig.5-e), the heteroclinic net (fig.5-f) as the set of the six Poincaré-map-images [26] of the unperturbed heteroclinic separatrix in the forward-time-direction and in the back-time-direction $t \to -\infty$ (six Poincaré-map-preimage). All of the simulations (fig.5) correspond to the oscillating chaos (fig.4-a) with the same DSSC parameters and the motion's initial conditions. So, the illustrations (fig.5) show us the appropriate features of the chaotic regime: the irregularity of the motion parameters (their time-history), the tangled polhode, and complicated heteroclinic nets.

5. The new approach of the realization of the chaos-free spinup maneuver

As it was indicated in the previous section, in order to the local heteroclinic chaos avoidance during the spinup maneuver we need to instantly translate the whole longitudinal angular momentum of the platform-body to the rotor-body (the instantaneous transition from the phase portrait fig.3-a/a' straight to the frame fig.3-h/h').

For the realization of this "jumping" change of the phase portraits' form (fig.3-a→fig.3-h) we can use the method of the conjugated rotors spinup-captures [39-41], which were developed for the multi-rotor spacecraft's attitude reorientation.

For application of this method to the chaos-free spinup maneuver we can add to the DSSC-two-body-coaxial-system the "opposite" rotor #3 (fig.6), which is conjugated to the rotor #1. Then it is possible to perform the "conjugate spinup" – this is the process of the spinup of the conjugated rotors in opposite directions up to desired values of the relative angular velocity with the help of internal torques; the summarized angular momentum of the conjugated rotors during the conjugate spinup is constant. Then, for the instantaneous transition of the angular momentum of one of the conjugate rotors to the main body (to compensate the angular momentum of the main body, and to stop it) we can make the «rotor capture» – it is the immediate stopping-deceleration of the rotor relative angular velocity with the help of internal torques. So, the rotor capture means the "instantaneous freezing" of the rotor with respect to the main body. The capture can be performed with the help of the gear meshing, large frictions or other methods.

To perform the spinup maneuver based on the new scheme we execute the following steps:

1). The DSSC is placed into the orbit in the "monobody" form (with the fixed rotors ## 1 and 3) with the initial value of the longitutinal angular velocity r_0.

2). The rotors-restrictions are removed and the rotors are exempted for the relative rotation.

3). The conjugated spinup of the rotors ## 1 and 3 is realized with the help of the following constant internal engines' torques:

$$M_1^i = \frac{(C_2 + C_3) r_0}{T_s}; \qquad M_3^i = -\frac{(C_2 + C_3) r_0}{T_s} \tag{5.1}$$

where C_3 is the axial inertia moment of the rotor #3; M_1^i - the internal torque of the rotor's #1 spinup engine; M_3^i - the internal torque of the rotor's #3 spinup engine; T_s – is the duration (time-moment) of the rotor's spinup. At the end of the spinup with the torques (5.1) the rotor #3 and the main body (#2) have the equal magnitudes of the longitudinal angular momentum, but with opposite signs.

4). The capture of the rotor #3 is performed, then the longitudinal angular momentums of the body #2 and the rotor #3 immediately compensate each other – it stops the rotation of the both bodies (## 2,3). After the capture of the rotor #3 its relative rotation is prohibited, and from this time-moment we can consider the bodies #2 and #3 as the new coupled platform-body.

The indicated four steps present the new spinup maneuver's scheme with the instant translation of the stabilizing longitudinal angular momentum to the rotor-body (rotor #1). This scheme avoids the heteroclinic chaos in the DSSC dynamics during the spinup maneuver realization.

Based on the material [39] we can reduce the motion equations of the multi-rotor system to the considered three-body case:

$$\begin{cases} A\dot{p} + (C - B) qr + q\Delta = 0; \\ B\dot{q} + (A - C) rp - p\Delta = 0; \\ C\dot{r} + \dot{\Delta} + (B - A) pq = 0; \end{cases} \quad \begin{cases} \dot{\Delta}_1 = M_1^i; \quad \dot{\Delta}_3 = M_3^i; \\ \dot{\Delta} = \dot{\Delta}_1 + \dot{\Delta}_3, \end{cases} \tag{5.2}$$

where

$$\Delta = \Delta_1 + \Delta_3; \quad \Delta_1 = C_1 (r + \sigma_1); \quad \Delta_3 = C_3 (r + \sigma_3)$$
$$A = A_1 + A_2 + A_3; \quad B = A_1 + B_2 + A_3; \quad C = C_2 \tag{5.3}$$

$diag[A_3, A_3, C_3]$ – the inertia tensor of the rotor #3 in the corresponding connected frames $Ox_3y_3z_3$; σ_1 – the rotor #1 relative angular velocity, σ_3 – the rotor #3 relative angular velocity; Δ – the rotors' summarized absolute longitudinal angular momentum.

Here it is needed to note that the internal torques of the rotors engines correspond to the two actions: the rotors spinup within time T_s, and the rotor #3 capture at the time-moment T_c. We can use in this task the following form of the engine-torques based on the Heaviside function:

$$M_1^i = \frac{(C_2 + C_3) r_0}{T_s} \left(H(t) - H(t - T_s) \right);$$
$$M_3^i = -\frac{(C_2 + C_3) r_0}{T_s} \left(H(t) - H(t - T_s) \right) - \nu \sigma_3 H(t - T_c); \tag{5.4}$$

where ν – is the coefficient of the large viscous friction for the fast capture modeling, $H(t)$ – is the Heaviside function.

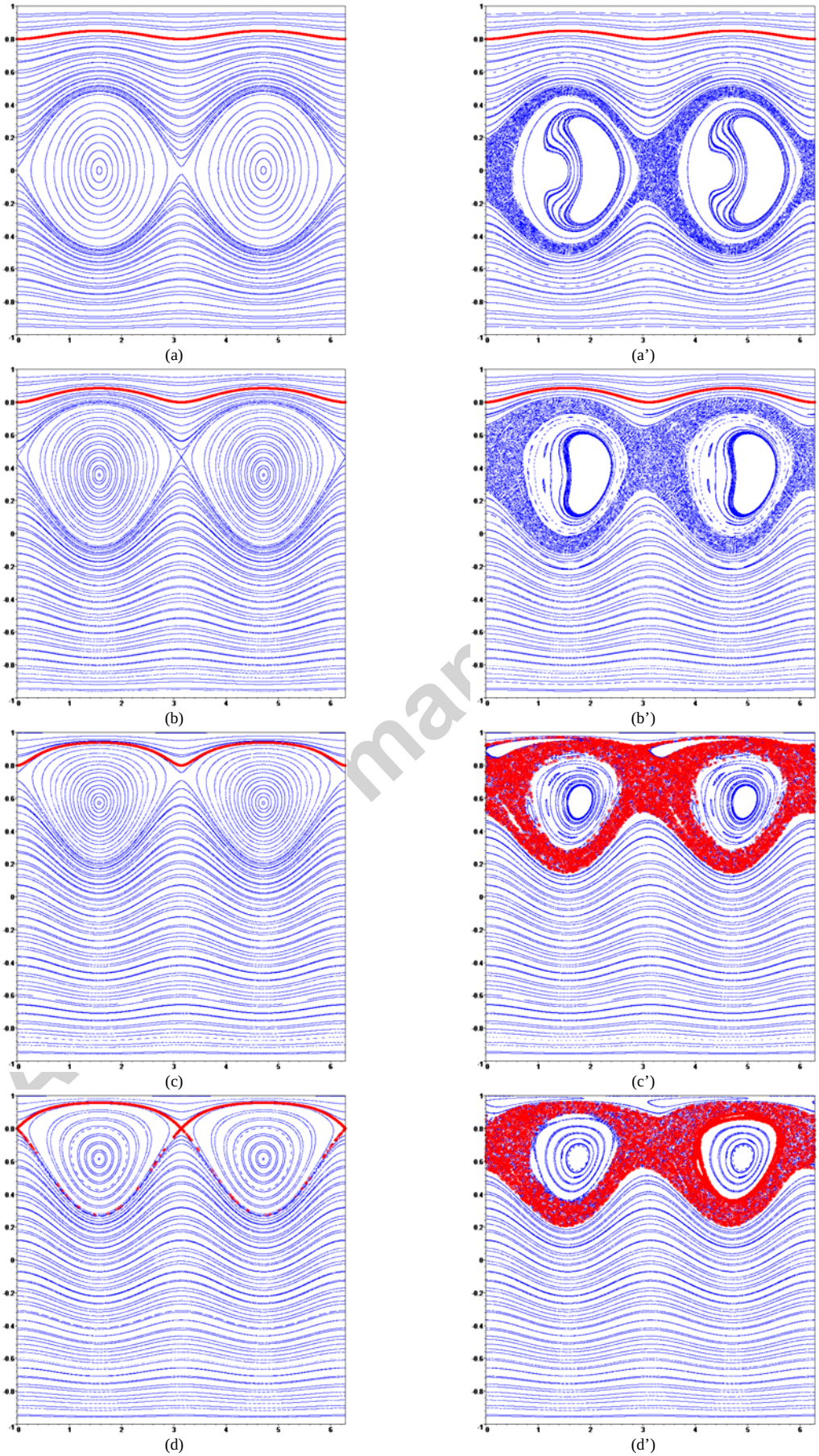

Fig. 3 *The frames of the phase portrait (start)*

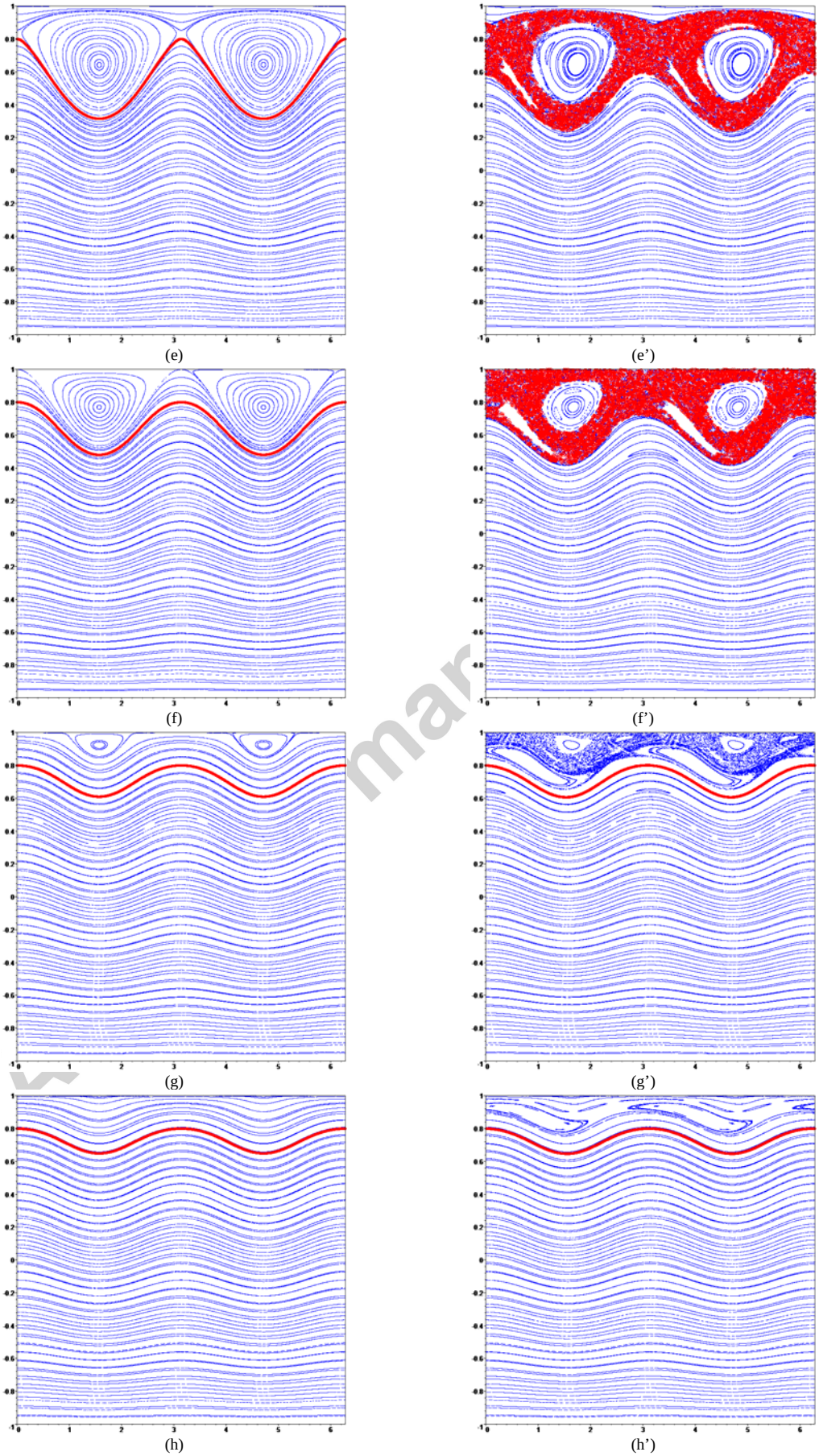

(e) (e') (f) (f') (g) (g') (h) (h')

Fig.3 *The frames of the phase portrait (finish)*

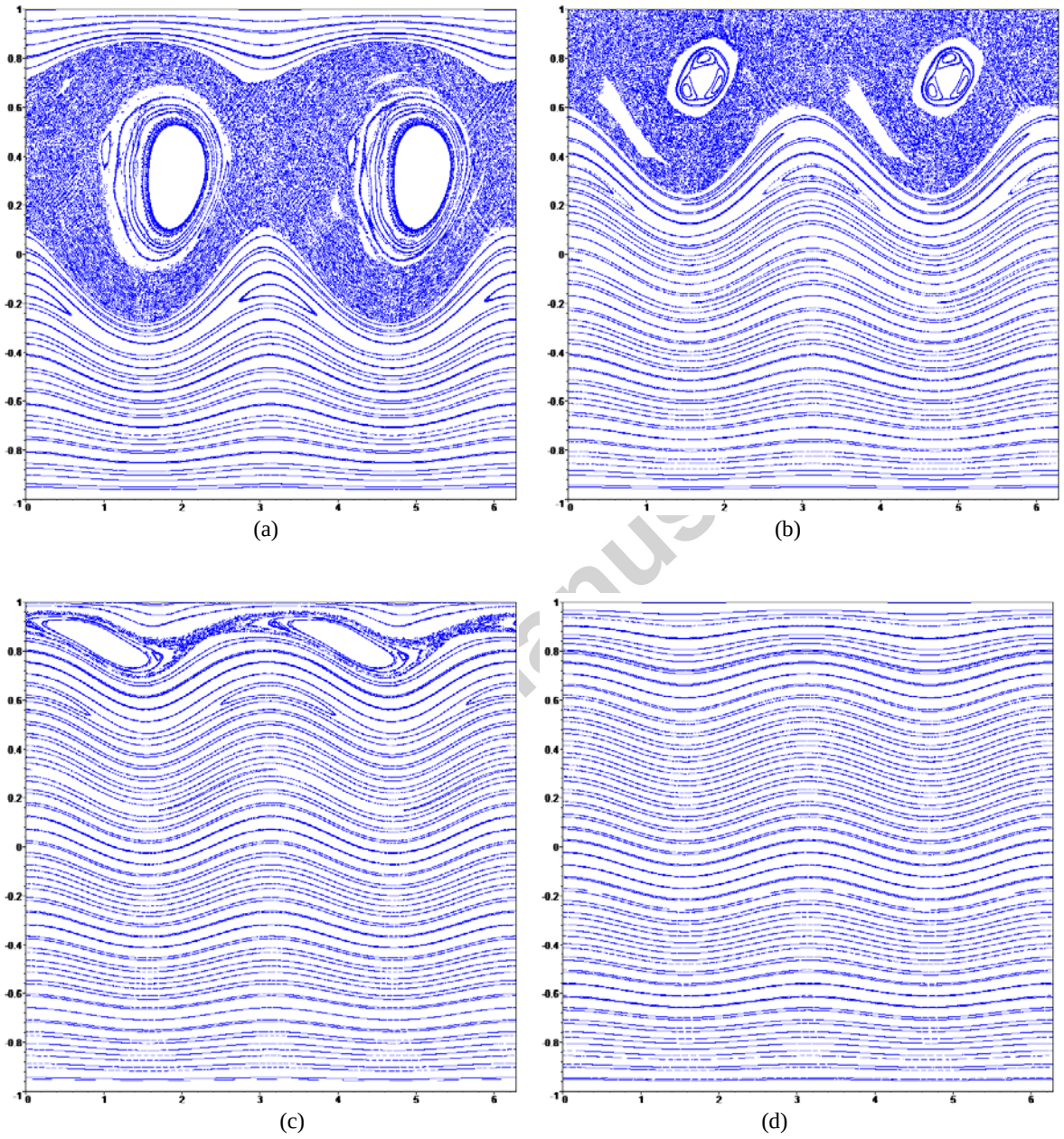

(a) (b)

(c) (d)

Fig.4 *Cases of chaos (in the system* (2.3)*)*:

(a) – the oscillating chaos $\left(\Delta = 4\right)$; (b) – the rotating chaos $\left(\Delta = \Delta^{*}\right)$;

(c) – the secondary heteroclinic chaos $\left(\Delta = \Delta^{**}\right)$; (d) – the disappearance of chaos $\left(\Delta = 0.9 I_2\right)$

$A_2 = 15,\ B_2 = 8,\ C_2 = 7,\ A_1 = 5,\ C_1 = 4;\quad I_2 = 20;\quad \overline{a}_1 = 1;\ \ \overline{a}_{2..N} = \overline{b}_{0..N} = 0;\quad \eta = 1/7;\quad \varepsilon = 0.6$

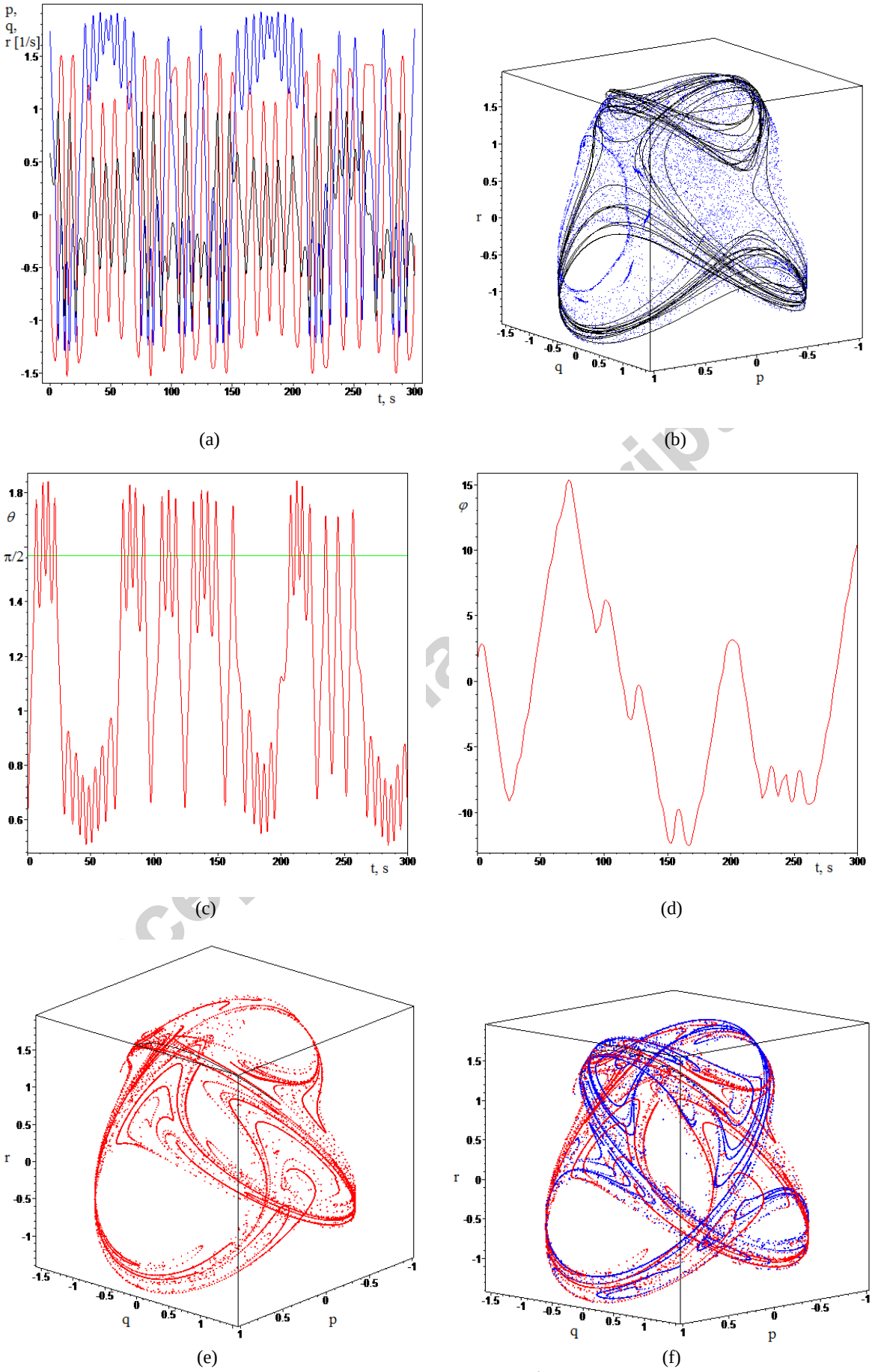

Fig.5 *The oscillating chaos' features*

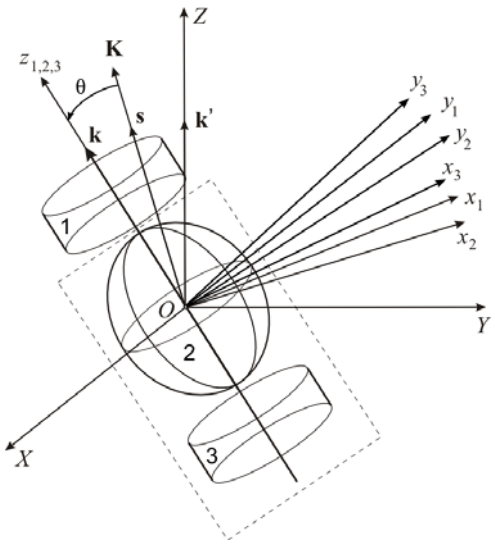

Fig.6 *The three-body DSSC*

The modeling results are presented at the fig.7. As we can see, the "jumping" change of the summarized longitudinal angular momentum Δ takes place at the time-moment T_c (fig.7-a), and the body-platform angular velocity *r* also immediately takes the zero-value (fig.7-b).

Here it is worth to note that the rotors ##1, 3 can be different in geometrical and inertia-mass parameters. This difference does not change the principle of the implementation of DSSC spinup maneuver. So, the rotor's #3 parameters can be selected based on the DSSC's constructive appropriateness.

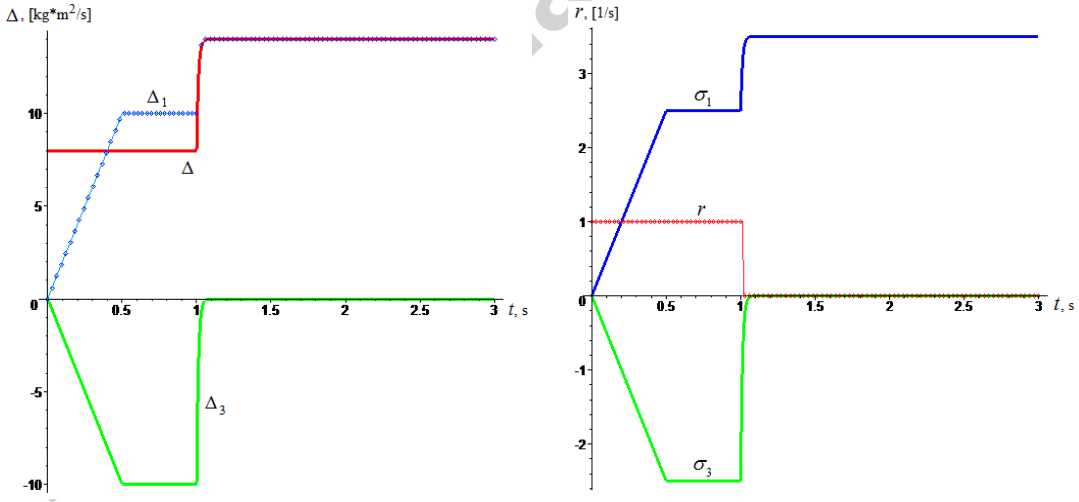

(a) (b)

Fig.7 *The DSSC's spinup maneuver modeling*:

$$A_2 = 15,\ B_2 = 8,\ C_2 = 6,\ A_1 = A_3 = 5,\ C_1 = C_3 = 4\ \left[\text{kg}\cdot\text{m}^2\right];$$

$$\nu = 200\ \left[\text{kg}\cdot\text{m}^2/\text{s}\right];\ \ r_0 = 1\,[1/\text{s}];\ \ T_s = 0.5,\ \ T_c = 1\ [\text{s}]$$

The considered spinup maneuver's scheme with instant translation of the stabilizing longitudinal angular momentum to the rotor-body (rotor #1) allows to avoid the heteroclinic chaos in the DSSC dynamics. This is possible due to the instant change of the phase portraits' form with the separatrix-region disappearance.

CONCLUSION

In the article the attitude dynamics of the dual-spin spacecraft was considered during the

classical spinup maneuver realization, including the investigation of the regimes of the heteroclinic chaos arising at the presence of polyharmonic perturbations. Also the classification of the possible cases of the DSSC chaotic regimes was implemented.

As it was shown, the main reason of the chaotic regimes' initiation is the qualitative changing of the phase portraits' structure during the classical spinup maneuver, when the gradually increasing of the Δ-value inside the interval $\left[C_1 r_0, L_0 = (C_1 + C_2) r_0\right]$ takes place. In this process the separatrix-region is moved up to upper border of the phase portrait, and, hence, the zone of the heteroclinic chaos (in its evolution) inevitably passes through the particular solution corresponding to the DSSC's attitude position, which is stabilized by the partial twist. So this "stabilized solution" is inevitably involved in the chaotic regime, and, therefore, the attitude orientation/stabilization can be lost.

Here we underline that the failures/anomalies facts indicated in the introduction-section correspond to the real "experimental data" [42-44] illustrating the irregular motion cases and phantom commands realization; but the comparison of this data with the theoretical results is problematic because the indicated failures were not being monitored. So, the special experiments for the chaos phenomena study were not conducted in the framework of the known DSSC space programs. The space programs' engineers/implementators ought to plan and conduct these interesting experiments in the near future.

To avoid the chaotic regimes initiation we suggested the new method of the spinup maneuver realization, which is based on the three-body-DSSC scheme with the execution of the conjugated rotors spinup-captures. This modified spinup maneuver provides the instant translation (the jump) between the phase portrait's forms with the separatrix-region disappearance, and, therefore, without any chaotic regime arising.

ACKNOWLEDGMENTS

This work was supported by the Russian Foundation for Basic Research (RFBR # 11-08-00794-a).

REFERENCES

[1] J. Wittenburg, Dynamics of Systems of Rigid Bodies. Stuttgart: Teubner, 1977.

[2] J. Wittenburg, Beitrage zur dynamik von gyrostaten, Accademia Nazional dei Lincei, Quaderno N. 227 (1975).

[3] Serret, J.A. Memoire sur l'emploi de la methode de la variation des arbitraires dans theorie des mouvements de rotations, Memoires de l'Academie des sciences de Paris, Vol. 35, 1866, pp. 585-616.

[4] H. Andoyer, Cours de Mecanique Celeste, Paris: Gauthier-Villars, 1923.

[5] A. Deprit, A free rotation of a rigid body studied in the phase plane, American Journal of Physics 35 (1967) 424– 428.

[6] E. Leimanis, The general problem of the motion of coupled rigid bodies about a fixed point. Berlin: Springer-Verlag, 1965.

[7] V.V. Kozlov, Methods of Qualitative Analysis in the Dynamics of a Rigid Body, Gos. Univ., Moscow, 1980.

[8] P. W. Likins, Spacecraft Attitude Dynamics and Control - A Personal Perspective on Early Developments, J. Guidance Control Dyn. Vol. 9, No. 2 (1986) 129-134.

[9] D. L. Mingori, Effects of Energy Dissipation on the Attitude Stability of Dual-Spin Satellites, AIAA Journal, Vol. 7, No. 1 (1969) 20-27.

[10] P. M. Bainum, P. G. Fuechsel, D. L. Mackison, Motion and Stability of a Dual-Spin Satellite With Nutation Damping, Journal of Spacecraft and Rockets, Vol. 7, No. 6 (1970) 690-696.

[11] K. J. Kinsey, D. L. Mingori, R. H. Rand, Non-linear control of dual-spin spacecraft during despin through precession phase lock, J. Guidance Control Dyn. 19 (1996) 60-67.

[12] C. D. Hall, Escape from gyrostat trap states, J. Guidance Control Dyn. 21 (1998) 421-426.

[13] C. D. Hall, Momentum Transfer Dynamics of a Gyrostat with a Discrete Damper, J. Guidance Control Dyn., Vol. 20, No. 6 (1997) 1072-1075.

[14] A. E. Chinnery, C. D. Hall, Motion of a Rigid Body with an Attached Spring-Mass Damper, J. Guidance Control Dyn. Vol. 18, No. 6 (1995) 1404-1409.

[15] C.D. Hall, R.H. Rand, Spinup Dynamics of Axial Dual-Spin Spacecraft, Journal of Guidance, Control, and Dynamics, Vol. 17, No. 1 (1994) 30–37.

[16] A.I. Neishtadt, M.L. Pivovarov, Separatrix crossing in the dynamics of a dual-spin satellite. Journal of Applied Mathematics and Mechanics, Volume 64, Issue 5, 2000, Pages 709-714.

[17] V.K. Melnikov, On the stability of the centre for time-periodic perturbations, Trans. Moscow Math. Soc. No.12 (1963) 1-57

[18] P. J. Holmes, J. E. Marsden, Horseshoes and Arnold diffusion for Hamiltonian systems on Lie groups, Indiana Univ. Math. J. 32 (1983) 273-309.

[19] M. Inarrea, V. Lanchares, Chaos in the reorientation process of a dual-spin spacecraft with time-dependent moments of inertia, Int. J. Bifurcation and Chaos. 10 (2000) 997-1018.

[20] Jinlu Kuang, Soonhie Tan, Kandiah Arichandran, A.Y.T. Leung, Chaotic dynamics of an asymmetrical gyrostat, International Journal of Non-Linear Mechanics, Volume 36, Issue 8 (2001) 1213-1233.

[21] E.A. Ivin, Decomposition of variables in task about gyrostat motion, Mathematics and Mechanics series, no.3, Vestnik MGU (Transactions of Moscow's University), 1985, Pp.69–72.

[22] Jianhua Peng, Yanzhu Liu, Chaotic motion of a gyrostat with asymmetric rotor, International Journal of Non-Linear Mechanics, Volume 35, Issue 3 (2000) 431-437.

[23] Z.-M. Ge, T.-N. Lin, Chaos, Chaos Control And Synchronization Of A Gyrostat System, Journal of Sound and Vibration, Volume 251, Issue 3 (2002) 519-542.

[24] K.H. Shirazi, M.H. Ghaffari-Saadat, Chaotic motion in a class of asymmetrical Kelvin type gyrostat satellite, International Journal of Non-Linear Mechanics, Volume 39, Issue 5 (2004) 785-793.

[25] A.V. Doroshin, Modeling of chaotic motion of gyrostats in resistant environment on the base of dynamical systems with strange attractors. Communications in Nonlinear Science and Numerical Simulation, Volume 16, Issue 8 (2011) 3188–3202.

[26] A.V. Doroshin, Heteroclinic dynamics and attitude motion chaotization of coaxial bodies and dual-spin spacecraft, Communications in Nonlinear Science and Numerical Simulation, Volume 17, Issue 3 (2012) 1460–1474.

[27] V.S. Aslanov, A.V. Doroshin, Chaotic dynamics of an unbalanced gyrostat. Journal of Applied Mathematics and Mechanics, Volume 74, Issue 5 (2010) 525-535.

[28] V. Volterra, Sur la théorie des variations des latitudes. Acta Math. 22 (1899).

[29] N.E. Zhykovski, On the motion of a rigid body with cavities filled with a homogeneous liquid. Collected works, 1, Moscow-Leningrad, Gostekhisdat, 1949.

[30] A. Elipe, V. Lanchares, Exact solution of a triaxial gyrostat with one rotor, Celestial Mechanics and Dynamical Astronomy, Issue 1-2, Volume 101, 2008, pp 49-68.

[31] I. Basak, Explicit solution of the Zhukovski-Volterra gyrostat, Regular and chaotic dynamics Vol.14, N.2 (2009) 223-236.

[32] V.S. Aslanov, Behavior of Axial Dual-spin Spacecraft, Proceedings of the World Congress on Engineering 2011, WCE 2011, 6-8 July, 2011, London, U.K., pp. 13-18.

[33] V.S. Aslanov, Integrable cases in the dynamics of axial gyrostats and adiabatic invariants, Nonlinear Dynamics, Volume 68, Numbers 1-2 (2012) 259-273.

[34] A.V. Doroshin, Exact solutions for angular motion of coaxial bodies and attitude dynamics of gyrostat-satellites. International Journal of Non-Linear Mechanics, Volume 50 (2013) 68-74.

[35] V.S. Aslanov, A.V. Doroshin, Stabilization of a reentry vehicle by a partial spin-up during uncontrolled descent. Cosmic Research 40 (2) , pp. 178-185.

[36] A.V. Doroshin, Evolution of the Precessional Motion of Unbalanced Gyrostats of Variable Structure. Journal of Applied Mathematics and Mechanics 72 (2008) 259–269.

[37] A.V. Doroshin, Synthesis of Attitude Motion of Variable Mass Coaxial Bodies. WSEAS TRANSACTIONS on SYSTEMS and CONTROL, Issue 1, Volume 3 (2008) 50-61.

[38] A.V. Doroshin, Analysis of attitude motion evolutions of variable mass gyrostats and coaxial rigid bodies system, International Journal of Non-Linear Mechanics, Volume 45, Issue 2 (2010) 193–205.

[39] A.V. Doroshin, Attitude Control of Spider-type Multiple-rotor Rigid Bodies Systems. Proceedings of the World Congress on Engineering 2009, London, U.K. Vol II, pp.1544-1549.

[40] A.V. Doroshin, Plenary Lecture 4: Attitude Dynamics and Control of Multi-Rotor Spacecraft and Roll-Walking Robots. Recent research in Communications, Electronics, Signal Processing & Automatic Control. – Proceedings of the 11th WSEAS International Conference on Signal Processing, Robotics and Automation (ISPRA'12). Cambridge, UK, 2012. P.15.

[41] A.V. Doroshin, Motion Dynamics of Walking Robots with Multi-Rotor Drive Systems. Recent research in Communications, Electronics, Signal Processing & Automatic Control. – Proceedings of the 11th WSEAS International Conference on Signal Processing, Robotics and Automation (ISPRA'12). Cambridge, UK, 2012. Pp.122-126.

[42] Satellite News Digest, Satellite Outages and Failures, 2013 (http://www.sat-nd.com/failures/).

[43] Spacecraft Anomalies Database Study // AEROSPACE REPORT NO. TR-95(5940)-1, 1994, Prepared by H. C. Koons, The Aerospace Corporation Technology Operations, El Segundo, CA 90245-4691.

[44] K.L. Bedingfield, R.D. Leach, and M.B. Alexander, Editor, Spacecraft System Failures and Anomalies Attributed to the Natural Space Environment / August 1996/ NASA Reference Publication 1390.

highlights

Attitude dynamics of a dual-spin spacecraft (DSSC) are considered.
Some regimes of the heteroclinic chaos are described.
The local chaotization of the DSSC is investigated at
the presence of polyharmonic perturbations.
Reasons of the chaotic regimes initiation at the spinup
maneuver realization are studied.
An approach for the local heteroclinic chaos escape at
the modification of the classical spinup maneuver is suggested.